Influence of ultrasonic treatment on heat transfer in the heat exchanger

Nihad Kamar, Marie Le Page Mostefa, Hervé Muhr, Pierre-Olivier Jost

Influence of ultrasonic treatment on heat transfer in the heat exchanger

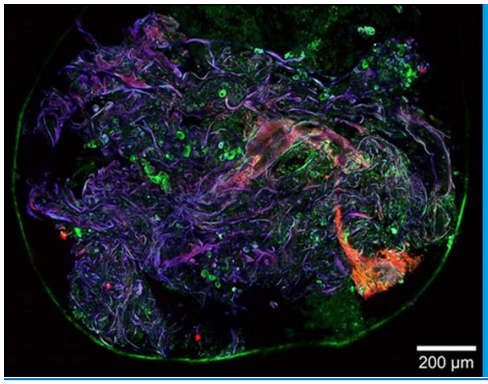

Journal of Physics Communications

PAPER

Influence of ultrasonic treatment on heat transfer in the heat exchanger

Nihad Kamar[1], **Marie Le Page Mostefa**[1], **Hervé Muhr**[1] and **Pierre-Olivier Jost**[2]

[1] University of Lorraine, Reactions and Process Engineering Laboratory (LRGP) UMR 7274 CNRS, 1 rue Grandville BP20451, 54001 Nancy, France

[2] Sofchem, 9 rue du Gué, 92500 Rueil Malmaison, France

E-mail: nihad.kamar@univ-lorraine.fr

Keywords: ultrasound, heat exchanger, piezoelectric transducer, heat transfer, global exchange coefficient, temperature profiles

OPEN ACCESS

RECEIVED
30 May 2022

REVISED
23 August 2022

ACCEPTED FOR PUBLICATION
16 September 2022

PUBLISHED
26 September 2022

Abstract

This paper deals with the influence of guided ultrasonic waves on heat transfer. Two piezoelectric transducers, whose structure can be vibrated at different powers and at their resonant frequency in the ultrasonic range of 27–45 kHz, were placed on the plates of a heat exchanger to inhibit the formation of a mineral deposit. These waves were set to diffuse only into the metal plates of the exchanger. During these tests, an increase in the heat transfer between the two fluids was directly observed on the continuous recording of the outlet temperature, on the calculations of the global exchange coefficient, and on the flow exchanged between the two fluids in the laminar regime. Tests are presented in this article, tests in the presence of the 45 kHz transducer, another with a 27 kHz transducer, and which combines the two have a different positioning on the exchanger. The results obtained from the ultrasonic guided waves are similar to the classical ultrasonic waves.

Nomenclature

English symbols

a	Thickness of the double envelope (m)
b	Spacing between turns (m)
C_p	Heat capacity in ($J.kg^{-1}.K^{-1}$)
D_H	Hydraulic diameter (m)
e_{CaCO3}	Limestone thickness (m)
H	Overall heat transfer coefficient ($W.m^{-2}.K^{-1}$)
$h_{.c.}$	Heat coefficient an cold side ($W.m^{-2}.K^{-1}$)
h_h	Heat coefficient an hot side ($W.m^{-2}.K^{-1}$)
$\dot{m}_c$	Mass flow rate of the cold fluid ($kg.s^{-1}$)
$\dot{m}_h$	Mass flow rate of the hot fluid ($kg.s^{-1}$)
Nu	Nusselt number (–)
Pr	Prandtl number (–)
Pr_p	Prandtl number at the wall (–)
P_{us}	Amount of heat generated by the ultrasonic power (W)
Q_m	Mass flow rate in $kg.s^{-1}$
Q_v	Volume flow in $l.min^{-1}$
q_c	Amount of heat acquired by the cold circuit (W)
q_{env}	Amount of heat lost to the environment (W)

q_h	Amount of heat released by the hot circuit (W)
Re	Reynolds number (–)
S	Exchange surface (m)
T_{ci}	Inlet temperature of the cold liquid in °C
T_{co}	Outlet temperature of the cold liquid in °C
T_{hi}	Inlet temperature of the hot liquid in °C
T_{ho}	Outlet temperature of the hot liquid in °C
V	Velocity of the liquid in ($m.s^{-1}$)
Geek symbols	
ρ	Density ($kg.m^{-3}$)
μ	Dynamic viscosity in (Pa.s)
Φ	Acquired heat flux in (W)
λ_p	The thermal conductivity of the plate material ($W.m^{-1}.K^{-1}$)
λ_{CaCO_3}	The thermal conductivity of calcium carbonate ($W.m^{-1}.K^{-1}$)
ΔT_{lm}	Temperature difference
Subscripts	
c	Cold
h	Hot
i	Inlet
o	Outlet
v	Volume
m	Masse
US	Ultrasonic
envi	environnement

Introduction

In industrial companies, the heat exchanger is an essential element of any energy management policy, 90% of the thermal energy used in industrial processes passes through a heat exchanger at least once [1]. The main problems encountered by heat exchanger users are related to fouling phenomena that reduce heat transfer.

Research is currently conducted on two completely different, but complementary, fronts for fouling detection [1].

The first method was developed by Zeljka Ujevic Andrijic *et al* it is a method based on neural network and nonlinear finite impulse response models, using the number of transfer units method, these models effectively detect fouling formation in an industrial heat exchanger [2]. The other model was created by C. B. Panchal and Ehr-Ping Huangfu, it is a model based on the calculation of the rate of the transfer resistance as a function of time to detect fouling [3].

And the second study, which we wish to join, concerns the products allowing the cleaning of these deposits, either during operation or during the maintenance sequence. Several experimental studies address the intensification of heat transfer by ultrasonic waves [4, 5].

Nakayama tested ultrasonic energy of 140 W with a frequency of 20 kHz on a 20 mm thick plate immersed in distilled water. He found up to four times an increase in heat transfer coefficient [6].

Y. Tisseau, P. Boldo, N. Gondexon, and A. Bontemps tested the effect of ultrasound on a beam-type heat exchanger, the results obtained showed that ultrasound systematically increases the overall heat transfer coefficient. However, this improvement is very sensitive to the hydrodynamic configuration chosen and does not vary with the power of the ultrasound field [7].

According to Nomura *et al* when ultrasonic vibration of 28 and 45 kHz was applied to water, the heat transfer coefficient increased significantly due to cavitation bubbles. However, when the ultrasonic vibration was close to 100 kHz, the increase in heat transfer coefficient became small compared to those of 28 and 45 kHz [8].

The same author tested the application of sound energy generated by a 60.7 kHz transducer on three types of the plate (acrylic, aluminum, and polystyrene) of different thicknesses, he found that the heat transfer coefficient

decreased as the thickness of the flat plate increased. And that the heat transfer coefficient was highest for the acrylic plate, then the aluminum plate, and lowest for the polystyrene plate [9].

In another study by the same author, a horizontal downward-facing heating surface with ultrasonic vibrations from below was performed in a natural convection region. Up to ten times more, heat transfer coefficient was obtained by applying 20 W in tap water and degassed water in the presence of a fixed horn transducer on resonance frequency 60.7 kHz [10].

An experimental investigation was conducted to investigate the effects of ultrasonic waves on heat transfer by Bartoli and Baffigi, under subcooled boiling conditions of distilled water. The acoustic flow influences the kinematic field and thus increases the heat transfer coefficient [11].

Monnot *et al* performed experiments using a specific experimental setup involving a high-frequency ultrasonic reactor equipped with a helical cooling coil, to study the effect of ultrasound at different frequencies on the heat transfer between the water contained in the reactor and the cooling water flowing through the coil. The results obtained show that the ultrasonic field leads to an increase in the cooling rate due to an increase in the overall heat transfer coefficient of the coil up to 100% [12].

In the same context, Gondrexon *et al* applied the low-frequency ultrasonic field on a shell and tube heat exchanger, the results show that under ultrasonic conditions, the overall heat transfer coefficient can be increased from 123 to 257% [13].

Experimental studies were carried out by Hoshino and Yakawa on a 28KHz standing ultrasonic wave applied to a sonoexchanger type heat exchanger. The results obtained show a good temperature distribution and a good heat transfer by free convection. The authors explained the heat transfer mechanism in an ultrasonic standing wave field by an acoustic radiation pressure theory (Hoshino and Yukawa 1979) [14].

A study by Komarov and Hirasawa aims to show the enhancement of heat transfer between solids and ambient gas by the application of strong acoustic fields. The experiments are carried out on a frequency range of 6.9 to 17.2 kHz. Examination of the Nusselt number with and without acoustic field shows that the heat transfer rate is improved with the intensity of the acoustic field. And the higher the gas flow velocity, the lower the effect of the sound wave on the heat transfer enhancement [15].

This heat transfer enhancement is different from one fluid to another, and depends on the substances present in the medium as well. The heat transfer enhancement for brine shows a different variation from that of sugar water, and the heat transfer enhancement ratio always increases with increasing sugar water concentration [16].

This is confirmed by Bonekamp and Bier in a study to show the effect of 40 kHz ultrasound on the free-boiling heat transfer of the refrigerant mixture R23 and R134a over a wide range of heat flows and saturation pressures. The improvement of the heat transfer coefficient, which can be achieved by 40 kHz ultrasound, is much more pronounced for mixtures than for single bodies, especially at medium saturation pressures. However, this improvement is limited to rather low heat flows ($q < 10\ kW\ m^{-2}$) [17].

The impact of ultrasound on heat transfer is related to the operating parameter. According to Bulliard-Sauret, the laminar regime is characterized by a remarkable difference between the overall exchange coefficients obtained without and with ultrasound, as shown in the figure below for a frequency of 35 kHz [4]. Figure 1 below shows two graphs. The first one deals with the variation of the global exchange coefficient in different flow regimes, and the second one gathers several points, each one representing a bibliographic reference. And this is also a study that shows an increase in heat transfer as a function of ultrasound frequency. Most of these studies deal with low frequency ultrasound and give roughly the same results.

On the other hand, Markov has performed experiments which show that the heat transfer coefficient can be up to double. In the case of a forced flow of a melt at high temperature under elastic oscillations at a frequency of 20 kHz [20]. In a previous study, our research team investigated the impact of ultrasonic guided waves on the formation of calcium carbonate within a heat exchanger. During experimental tests, an improvement in heat transfer was noticed [21]. In the classical ultrasonic techniques mentioned before, the waves propagate as mass waves. Mass waves can be in the form of compressional or shear motion of particles in the medium. They usually travel at a constant speed and the pulses are launched with a wide frequency spectrum. Conversely, a scattered acoustic wave can be defined as a guided acoustic wave transmitted by a process that limits the physical dispersion along the direction of propagationThe most important difference between conventional ultrasound and guided waves is the variation in velocity with the change in frequency The objective of our study is to compare the heat transfer realized in a heat exchanger with insulated plates and joints, in the presence or not of guided ultrasonic waves at a fixed frequency, at two different ultrasonic powers. And to realize the two temperature profiles in real time with the casteminus and to approve the effectiveness of these waves to improve the thermal transfer. The most important difference between conventional ultrasound and guided waves is the variation of speed with the change of frequency.

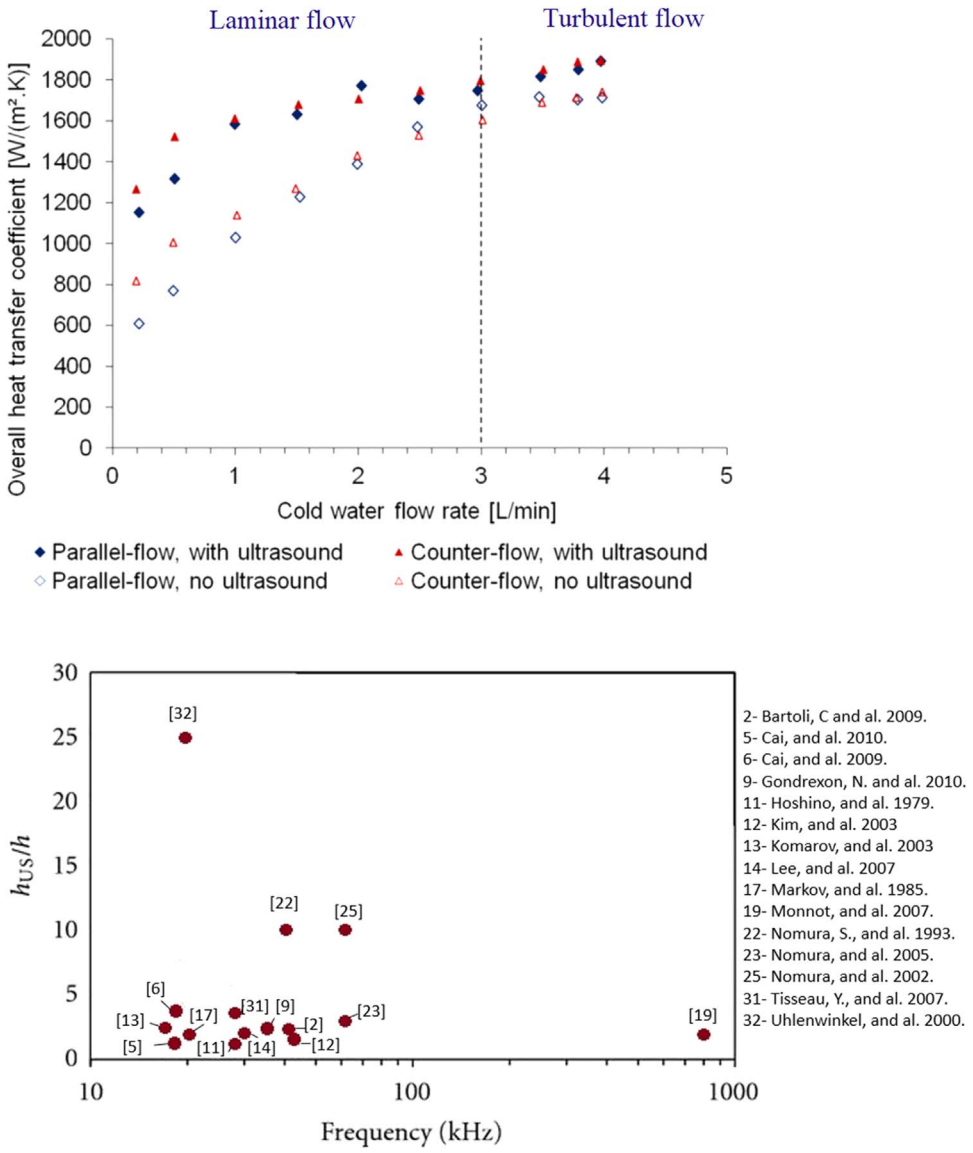

Figure 1. Evolution of the global heat exchange coefficient as a function of the cold fluid flow rate for a hot fluid flow rate fixed at 1.6 l min^{-1} in a coaxial exchanger [18], and Influence of ultrasonic frequency on the exchange coefficient h [19].

Materials and methods

Operating protocol

First, it is necessary to describe the experimental pilot studied and the quantities involved in the heat balances.

The experimental pilot

To study the effect of ultrasonic guided waves associated with the heterodyne effect of multiple frequencies on the formation of a mineral deposit ⟨calcium and magnesium carbonate⟩, an experimental pilot is designed ⟨see figure 2⟩. It includes:

- a plate and gasket heat exchanger, see figure 4, with an exchange surface of 0,38 m^2 ⟨10 plates, 5 compartments⟩, perfectly insulated with a cover based on glass wool.
- a cold circuit in which circulates, the scaling water ⟨total hardness of 30 °F⟩, stored in a tank ⟨100 l⟩, with a flow rate of 1.16 l.min^{-1} and an inlet temperature close to 25 °C,
- the hot circuit with 20 liters of ultrapure water at 50 °C and circulating at a flow rate of 16 l.min^{-1}.
- thermocouples are installed at each inlet and outlet of the exchanger in order to follow the heat exchange between the two fluids [21].

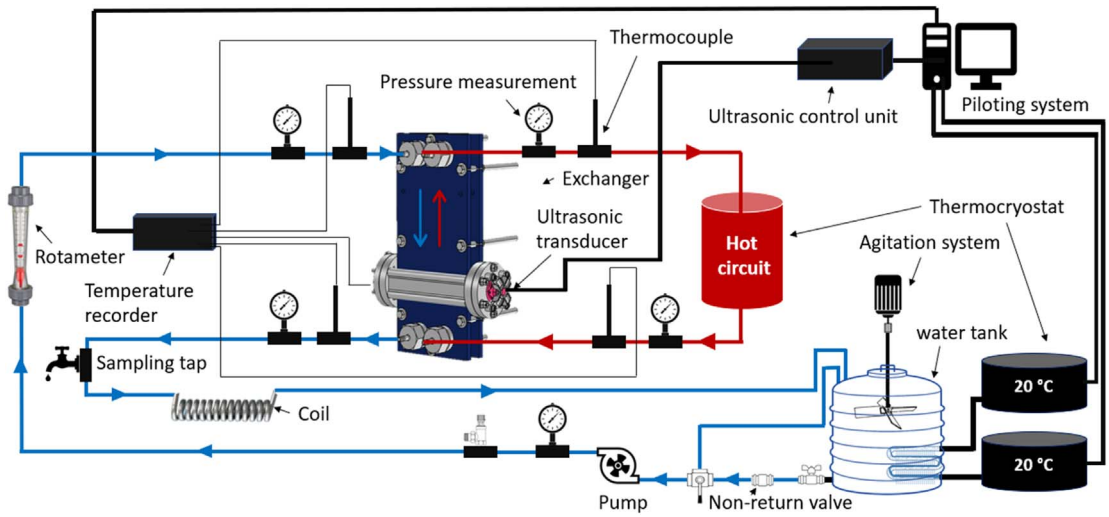

Figure 2. Description of the experimental set-up in the presence of the 45 kHz ultrasonic transducer [21].

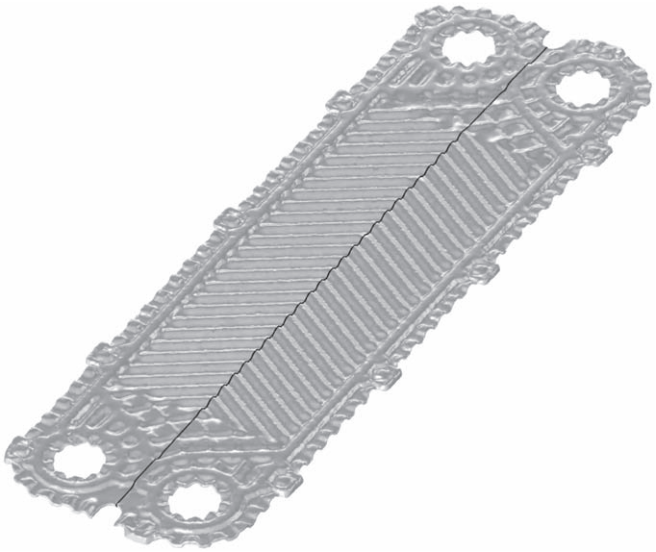

Figure 3. The geometry of the exchanger plate.

The exchanger plates

The plates of this exchanger are 316 L steel plates separated by a nitrile gasket. The plate is 460 mm long, 200 mm wide, and has a spline angle of approximately 60°, as shown in figure 3. The thickness of the plate is 0.5 mm and the space between the plates varies between 5 and 6 mm [22].

The ultrasonic transducer

In the present case, ultrasound is generated by a piezoelectric transducer of the Langevin type. In this kind of transducer, two polarized ferroelectric ceramics convert electrical energy into kinetic energy. The upper part of the ceramic is the counter mass, and the lower part is the horn 'transducer head' [23], as shown in figure 4.

When the two 'piezo' disks of the transducer absorb electrical energy through two electrodes, they convert it into kinetic energy, which causes a deformation/expansion of the piezoelectric materials. This expansion/displacement is transmitted to the radiant heat of the 'transverse vibration' transducer. And the larger the displacement amplitude of the radiating head, the higher the voltage [4].

In conventional ultrasonic techniques, the waves propagate as mass waves in the whole of the ultrasound scanner, whereas the ultrasound waveguides propagate mainly in the metal plates of the scanner. The objective of this approach is not to generate high levels of acoustic pressure, leading to cavitation, but rather to maximize

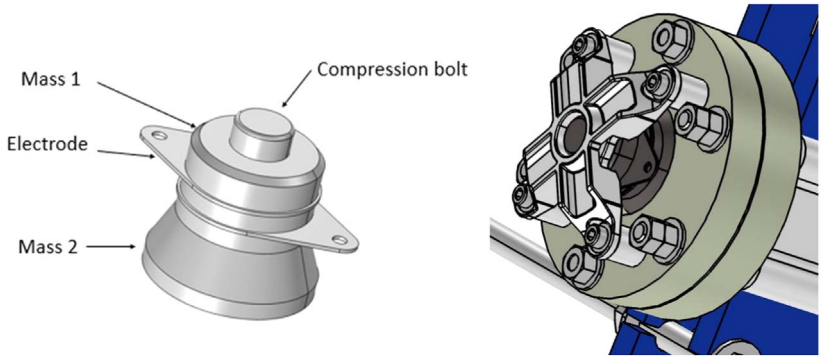

Figure 4. Fastening of the piezoelectric ceramics on the exchanger plates.

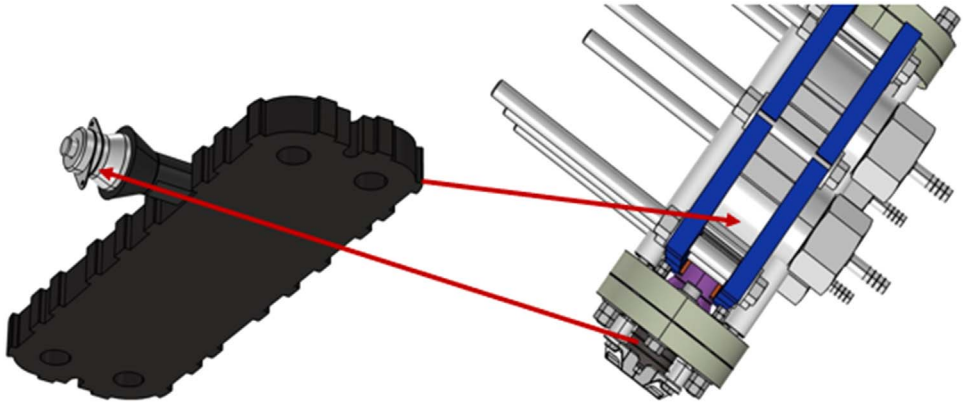

Figure 5. The 45 kHz transducer in contact with all plates of the exchanger.

the displacement at the exchange surface. These transducers have resonance frequencies where they have maximum gain.

The positioning of the ultrasonic transducer on the exchanger plates requires the placement of an intermediate metal piece, which ensures the transmission of the ultrasonic guided waves just in all the plates but not in the whole installation,, as shown in figure 5.

In past research studies, both 45 kHz and 27 kHz at medium power have shown encouraging results in inhibiting tartar formation. In this paper, the effect of two piezo-electric transducers, 45 kHz and 27 kHz, programmed on different ultrasonic powers will be tested to show the influence of ultrasound on heat transfer.

Method of evaluating the impact of scaling on the overall exchange coefficient

Two methods are considered in this manuscrite to estimate the influence of scaling on heat exchange performance.

The first method consists in considering the hydrodynamic behavior of the exchanger. For the same flow rate, the reduction of the hydraulic diameter of the exchanger resulting from the formation of a deposit creates an increase in the head losses [24]. In our case, no increase in pressure drop is detected: the operating mode ⟨closed-circuit⟩ and the duration of the experiment do not allow the formation of a sufficient scale thickness.

The second method is based on the measurement of the global heat transfer coefficient from a heat balance:

$$\phi = HS\Delta T_{ml} \tag{1}$$

With, ϕ, the flow exchanged between the two fluids (W); H, the overall heat transfer coefficient (W.m^{-2}.K^{-1}); S, the exchange surface of the exchanger (m^2); ΔT_{ml}, the logarithmic mean temperature difference between the fluids (K).

The heat flux lost by the hot fluid is written:

$$\phi = \dot{m}_h C_{ph}[T_{hi} - T_{ho}] \tag{2}$$

With, C_{ph}, the heat capacity of the hot fluid (J.kg^{-1}.K^{-1}) ; $\dot{m}_h$, mass flow rate of the hot fluid (kg.s^{-1}); T_{hi}, the inlet temperature of the hot fluid; T_{ho}, the outlet temperature of the hot fluid.

The system being insolated, it can be considered as adiabatic. Thus, the heat flow lost by the hot fluid is recovered by the cold fluid according to the following equation.

$$\phi = \dot{m}_c C_{pc}[T_{co} - T_{ci}] \tag{3}$$

With, C_{pc}, the mass heat capacity of the cold fluid (J.kg^{-1}.K^{-1}); $\dot{m}_c$, the mass flow rate of the cold fluid (kg.s^{-1}); T_{ci}, the inlet temperature of the cold fluid; T_{co}, the outlet temperature of the cold fluid.

The overall thermal exchange coefficient, H (W.m^{-2}.K^{-1}), reflects the capacity of the exchanger to transfer heat from the hot fluid to the cold fluid, as shown in the equation below:

$$\phi = HS\Delta T_{ml} \Leftrightarrow H = \frac{\phi}{S\Delta T_{ml}} \tag{4}$$

Note that the exchanger operates in counter-current and thus, ΔT_{ml} is calculated from the outlet and inlet temperatures of the hot and cold fluids according to the following equation:

$$\Delta T_{ml} = \frac{(T_{hi} - T_{co}) - (T_{ho} - T_{ci})}{\ln\left(\frac{T_{hi} - T_{co}}{T_{ho} - T_{ci}}\right)} \tag{5}$$

The overall heat transfer coefficient H can also be calculated for plate heat exchangers using the following formula:

$$\frac{1}{H} = \frac{1}{h_c} + \frac{e_{CaCO_3}}{\lambda_{CaCO_3}} + \frac{e_p}{\lambda_p} + \frac{1}{h_h} \tag{6}$$

With, h_c, the cold side heat coefficient (W.m^{-2}.K^{-1}); h_h, the hot side heat coefficient (W.m^{-2}.K^{-1}); ^{e}p, the thickness of the plate (m); λ_p, the thermal conductivity of the plate material (W.m^{-1}.K^{-1}); e_{CaCO_3}, the thickness of the calcium carbonate deposit (m); λ_{CaCO_3}, the thermal conductivity of calcium carbonate (W.m^{-1}.K^{-1}).

However, the heat transfer coefficients on the hot and cold sides of the heat exchanger can vary over time [25]. Therefore, the uncertainty of the overall heat transfer coefficient has been calculated by the following relationship [26]:

$$\frac{\mathrm{dH}}{\mathrm{H}} = \sqrt{\left(\frac{\mathrm{dQ}}{\mathrm{Q}}\right)^2 + \left(\frac{\mathrm{d}\Delta \mathrm{T_{LM}}}{\Delta \mathrm{T_{LM}}}\right)^2}$$

The proposed correlations for calculating the hot and cold side heat coefficients depend primarily on the plate geometry and corrugation angle. In this case, the plate surface is nonlinear, the wall temperature is assumed to be uniform, the spline shape is an 'obtuse' chevron with a corrugation angle α of 60°, and the overall exchange area is 0.38 m^2. The flow regime is determined from the Reynolds number Re:

$$R_e = \frac{\rho u D_H}{\mu} \tag{7}$$

With, ρ, the density of the fluid (kg.m^{-3}); μ, the dynamic viscosity of the fluid (Pa.s); D_H, the hydraulic diameter (m); u, the velocity of the fluid (m.s^{-1}).

The Nusselt number Nu is calculated by the following relation [27]:

$$\mathrm{Nu} = aRe^{b}Pr^{0,33}\left(\frac{Pr}{Pr_p}\right)^{0,33} \tag{8}$$

With, Re, the Reynolds number; Pr, the Prandtl number; ^{Pr}p, the Prandtl number at the wall.

The Prandtl number Pr is defined by:

$$Pr = \frac{\mu C_p}{\lambda} \tag{9}$$

With, ^{C}p, the heat capacity (J.kg^{-1}.K^{-1}); μ, the dynamic viscosity (Pa.s); λ, the thermal conductivity (W.m^{-1}.K^{-1}).

In the present case, the corrugation angle α of the plate is about 60°, see table 1.

Thus, it will be possible, by measuring the inlet and outlet temperatures of the fluids, and knowing the flow rates, to calculate the global exchange coefficient H, as well as estimate the average thickness of the scale formed.

Using the formula of the global exchange coefficient, we have:

$$\frac{1}{H} = \frac{1}{h_c} + \frac{e_{CaCO_3}}{\lambda_{CaCO_3}} + \frac{e_p}{\lambda_p} + \frac{1}{h_h} = \frac{S\Delta T_{ml}}{\phi} \tag{10}$$

Table 1. Variation of the coefficients a and b as a function of the corrugation angle α [27].

α	a	b	Re
60°	0.287	0.705	From 45 to 13 200

Table 2. Parameters for the calculation of the thermal conductivity with the previous equation [28].

i	C_i	d_i
1	0.802 01	−0.32
2	−0.259 92	−5.7
3	0.100 24	−12.0
4	−0.032 005	−15.0

Table 3. The coefficients and exponents a_i and b_i [28].

i	a_i	b_i
1	280.68	−1.9
2	511.45	−7.7
3	61.131	−19.6
4	0.459 03	−40.0

$$\Leftrightarrow e_{CaCO_3} = \lambda_{CaCO_3}\left(\frac{S\Delta T_{ml}}{\phi} - \frac{e_p}{\lambda_p} - \frac{1}{h_h} - \frac{1}{h_c}\right) \tag{11}$$

The thermal conductivity was calculated by the following relationship:

$$\lambda = \sum_{i=0}^{4} C_i (T^*)^{d_i} \tag{12}$$

Where, $T^* = \frac{T}{300\ \mathrm{K}}$ and the coefficients and exponents ai and bi are given in the table 2 [28].

$$\mu = (10^{-6}\mathrm{Pa.s})\sum_{i=0}^{4} a_i (T^*)^{b_i} \tag{13}$$

Where $T^* = \frac{T}{300\ \mathrm{K}}$ and the coefficients and exponents ai and bi are given in the table 3 [28]

The molar heat capacity of liquid water [29] is expressed by the following relation:

$$C_{\text{PL-mol}} = 72.43 + 0.0104\ \mathrm{T} \tag{14}$$

With, T in K with 278 K < T < 418 K; $C_{\text{PL-mol}}$ in J mol−1 K−1.

The calculation of the density of water was done by the following relation [29] :

$$\rho_{\mathrm{L}} = \frac{\mathrm{A}}{\mathrm{B}^{1+(1-\mathrm{T/C})^{\mathrm{D}}}} \tag{15}$$

With, ρL, in kg.m^{-3}; T in K with 273 K < T < 648 K.

Table 4 collects the coefficients A, B, C and D.

Logarithmic mean temperature difference (LMTD)

To know the temperature Th and Tc in an interval *dx* inside the exchanger and at time t, an equation has been developed for plotting the temperature profiles.

Figure 6 shows the flow of both hot and cold fluids between the plates.

The differential heat balance is expressed by the following relationship:

$$d\phi(x) = HdS\ [T_h(x) - T_c(x)] \tag{16}$$

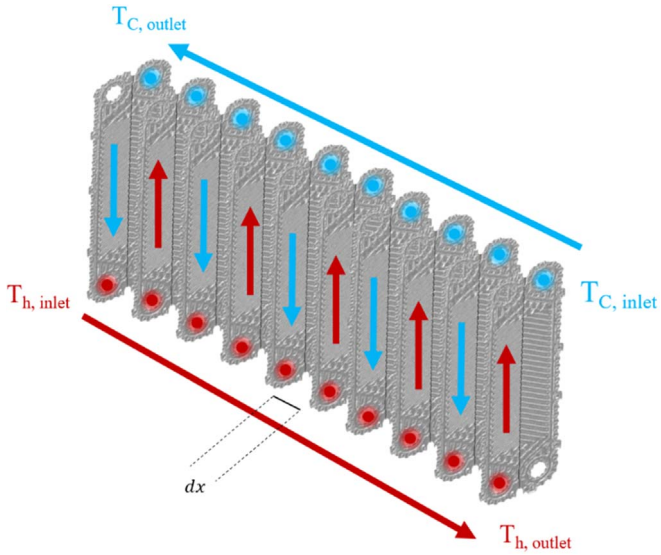

Figure 6. Heat transfer between the two fluids cold and hot throughout the plate assembly.

Table 4. Coefficients A, B, C and D for calculating density [29].

A	B	C	D
0.143 95	0.0112	649.727	0.051 07

With, (x) the infinitesimal heat flux transferred to the point of abscissa x (W); dS, the infinitesimal area (m^2).

$$d\phi(x) = \dot{m}_h C_{ph} dT_h \tag{17}$$

$$d\phi(x) = \dot{m}_c C_{pc} dT_c \tag{18}$$

$$\Leftrightarrow -\frac{HS}{L}[T_h(x) - T_c(x)]dx = \dot{m}_h C_{ph} dT_h \tag{19}$$

$$\Leftrightarrow \frac{HS}{L}[T_h(x) - T_c(x)]dx = \dot{m}_c C_{pc} dT_c \tag{20}$$

The exchange surface is 0.38 m^2, distributed over 10 plates. The distance between the first plate and the last plate is represented by a ratio of distance between 0 and L, as shown in the figure 7:

The equation (20) becomes:

$$\Leftrightarrow dT_h(x) = -\left(\frac{HS}{L\dot{m}_h C_{ph}}\right)[T_h(x) - T_c(x)]dx \tag{21}$$

$$\frac{dT_h}{dx}(x) = -\frac{HS[T_h(x) - T_c(x)]}{L(\dot{m}_c C_{pc})} < 0 \tag{22}$$

$$\frac{dT_c}{dx}(x) = \frac{HS[T_h(x) - T_c(x)]}{L(\dot{m}_h C_{ph})} > 0 \tag{23}$$

$$\Leftrightarrow dT_h(x) - dT_c(x) = \frac{HS(T_h - T_c)}{L}\left(\frac{1}{\dot{m}_c C_{pc}} - \frac{1}{\dot{m}_h C_{ph}}\right)dx \tag{24}$$

$$\int_{(T_h - T_c)_{x=0}}^{(T_h - T_c)_x} \frac{d(T_h - T_c)}{(T_h - T_c)} = \int_{x=0}^{x} \frac{HS}{L}\left(\frac{1}{\dot{m}_c C_{pc}} - \frac{1}{\dot{m}_h C_{ph}}\right)dx \tag{25}$$

$$\Leftrightarrow (Ln(T_h - T_{fc}))_{(T_h - T_c)_{x=0}}^{T_h - T_c} = \frac{HS}{L}\left(\frac{1}{\dot{m}_c C_{pc}} - \frac{1}{\dot{m}_h C_{ph}}\right)x \tag{26}$$

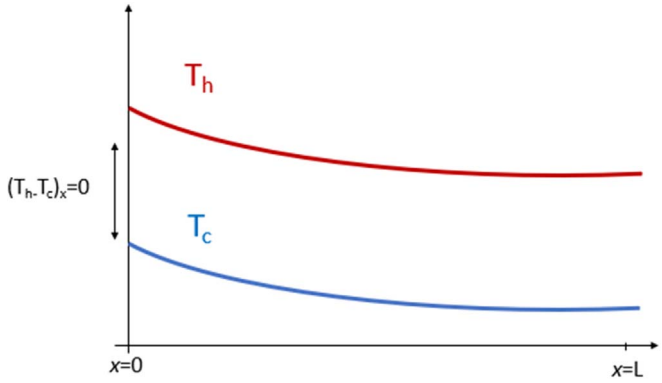

Figure 7. Graphical representation of a counter-current temperature profile.

Therefore, the equation of the temperature profile curve from (T_h and T_c)$_0$ becomes:

$$\Leftrightarrow (T_h - T_c)_x = (T_h - T_c)_{x=0} e^{\frac{HS}{L}\left(\frac{1}{\dot{m}_c C_{pc}} - \frac{1}{\dot{m}_h C_{ph}}\right)x} \tag{27}$$

for a distance ratio of: $0 < x < L$

Results and discussion

Fluid temperature monitoring

Temperature profiles

To better follow the heat exchange between the two compartments of the exchanger, a temperature profile was made for both fluids according to the following equation:

$$Ln\frac{\Delta T}{\Delta T_0} = \frac{HS}{L\dot{m}Cp}\, x \tag{28}$$

The following equation was plotted based on the temperature recording at each inlet and outlet of the exchanger for 72 h:

$$T_c - T_f = (T_{h0} - T_{c0}) e^{\left(\frac{1}{\dot{m}_h C_{ph}} - \frac{1}{\dot{m}_c C_{pc}}\right)\frac{HS}{L}x} \tag{29}$$

Without ultrasonic treatment

Figure 8 show the temperature recording at the cold and hot sides of the heat exchanger for 72 h without ultrasonic treatment.

The equation for the evolution of the final temperature in the absence of ultrasound is as follows, [19]:

$$T_{final} = \left(\frac{\dot{m}_h C_{ph} T_{hi} + \dot{m}_c C_{pc} T_{ci}}{\dot{m}_h C_{ph} + \dot{m}_c C_{pc}}\right) \tag{30}$$

With treatment ultrasonic

The figures 9, 10 show the experimental results of two tests in the presence of the ultrasonic treatment.

Mathieu Legay approved that in the presence of ultrasonic guided waves, the ultrasonic power intervenes in the energy balance, the equation of the final temperature Tfinal is expressed as follows [19]:

$$T_{final} = \left(\frac{\dot{m}_h C_{ph} T_{hi} + \dot{m}_c C_{pc} T_{ci}}{\dot{m}_h C_{ph} + \dot{m}_c C_{pc}}\right) + \left(\frac{P_{us}}{\dot{m}_h C_{ph} + \dot{m}_c C_{pc}}\right) \tag{31}$$

With,

P_{us}, the amount of heat generated by the ultrasonic power (W).

The same author approved that the factor responsible for the final temperature increase is defined by the following relationship:

$$\Delta T_{us} = \frac{P_{us}}{\dot{m}_h C_{ph} + \dot{m}_c C_{pc}} \tag{32}$$

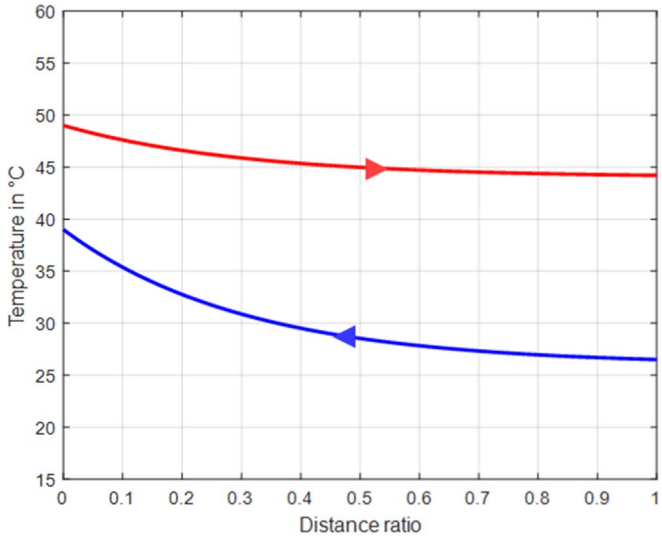

Figure 8. Temperature profile in absence of ultrasonic treatment, cold fluid (blue) and hot fluid (red).

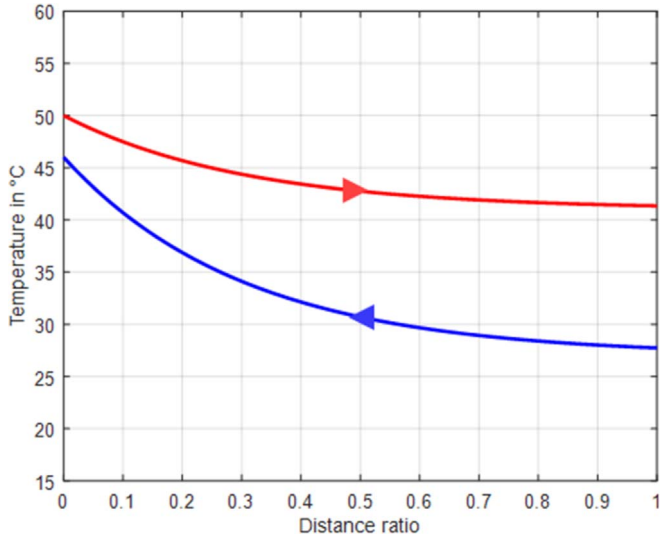

Figure 9. Temperature profile in the presence of the ultrasonic transducer programmed on a 15 W power, cold fluid (blue) and hot fluid (red).

The analysis of the temperature profiles shows that in the presence of the 30 W ultrasound, the final temperature is higher than that without ultrasound. The ultrasonic power contributes to the decrease of the gap between the two curves T_h and T_c, and thus contributes to the increase of the heat transfer.

Influence of scaling on the overall exchange coefficient

The results for the two compartments with and without ultrasonic treatment are shown in tables 5 and 6.

The variation of the logarithmic mean between the two fluids is 13.61 K. Therefore, the heat flux exchanged between the two fluids in the presence of the deposit is around: 3518 W, with an average thickness of about 9 μm.

The thickness of the deposit was measured experimentally with a 3D digital microscope after the dismantling of the exchanger [21], but the analysis of the scaled plates shows that the thickness of the deposit is not homogeneous since there are places that are sensitive to scale formation [22].

The global exchange coefficient in the absence of scale is: 1126 $W.m^{-2}.K^{-1}$

The variation of the logarithmic mean between the two fluids is 7.98 K. Therefore, the heat flux exchanged between the two fluids in the presence of the deposit is around: 6077 W, with an average scale thickness of about 2 μm.

The global exchange coefficient in the absence of scale is: 3458 $W.m^{-2}.K^{-1}$

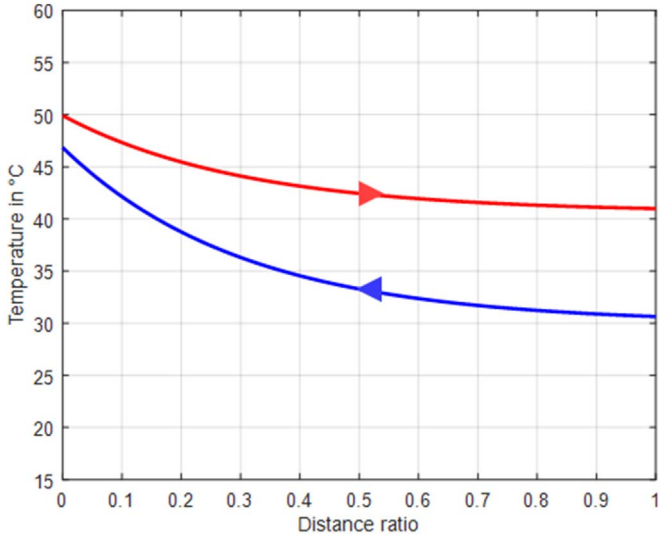

Figure 10. Temperature profile in the presence of the ultrasonic transducer programmed on a 30 W power, cold fluid (blue) and hot fluid (red).

Table 5. Calculation of heat transfer coefficients in the absence of ultrasonic treatment.

Compartments T (°C)	Cold rating (heat acquired)		Hot rating (waste heat)	
	$T_{ci} = 26 \pm 3$	$T_{co} = 39 \pm 4$	$T_{hi} = 49 \pm 1$	$T_{ho} = 44 \pm 3$
Qv (l.min^{-1})	1.67		16	
Q_m (kg.s^{-1})	0.03		0.26	
V (m.s^{-1})	0.01		0.07	
Φ(W)	1508		5527	
Cp (J.Kg^{-1}. K^{-1})	4200.5		4208.6	
ρ (Kg.m^{-3})	994.17		985.05	
μ (Pa.s)	$7{,}57 \times 10^{-4}$		$5{,}80 \times 10^{-4}$	
Re (laminar regime)	37		345	
λ (W.m^{-1}.K^{-1})	0.62		0.64	
Pr	6.75		6.58	
Nu	6.81		32.9	
a	0.29		0.29	
b	0.71		0.71	
h(W.m^{-2}.K^{-1})	826		4123	

Table 6. Calculation of heat transfer coefficients in the presence of the ultrasonic treatment (15 power).

Compartments Temperature (°C)	Cold rating (heat acquired)		Hot rating (waste heat)	
	$T_{ci} = 27 \pm 2$	$T_{co} = 46 \pm 3$	$T_{hi} = 50 \pm 0.2$	$T_{ho} = 41 \pm 3$
Qv (l.min^{-1})	1.67		16	
Qm(kg.s^{-1})	0.03		0.26	
V(m.s^{-1})	0.01		0.07	
Φ (W)	2199		9954	
Cp (J.Kg^{-1}. K^{-1})	4202.8		4208	
ρ (kg m^{-3})	991.6		985.7	
μ (Pa.s)	6.98×10^{-4}		5.9×10^{-4}	
Re (laminar regime)	36.53		345.7	
λ (W.m^{-1}.K^{-1})	0.63		0.64	
Pr	6.68		6.60	
Nu	6.79		32.96	
a	0.29		0.29	
b	0.71		0.71	
h (W.m^{-2}.K^{-1})	832		4119	

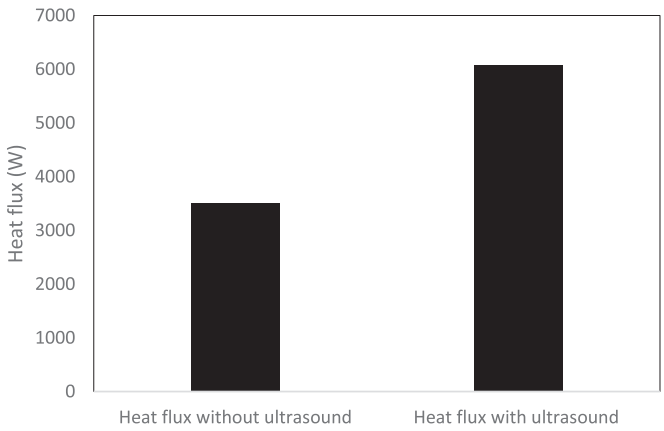

Figure 11. Variation of the heat flux exchanged between the two fluids in the absence and presence of ultrasound.

The energy balance of the two tests is simply the equality of the hot and cold flows. In this study, even if the exchanger is protected by an insulating cover, it is never perfectly adiabatic. Therefore, the energy balance becomes:

$$q_h = q_c + q_{env} \tag{33}$$

With, q_h, the amount of heat released by the hot circuit; q_c, the amount of heat acquired by the cold circuit; q_{env}, the amount of heat lost to the environment.

In the presence of ultrasound, the ultrasonic power is counted positive in the direction entering the system, the balance becomes:

$$q_h + P_{us} = q_c + q_{env} \tag{34}$$

With, q_h, the amount of heat released by the hot circuit; P_{us}, the amount of heat generated by the ultrasonic power; q_c, the amount of heat acquired by the cold circuit; q_{env}, the amount of heat lost to the environment.

Figures 11 and 12 show the variation of the exchanged fluxes and of the global thermal exchange coefficient in the presence and absence of ultrasound.

The results presented show that in the presence of ultrasound, an increase in the overall exchange coefficient and the heat flux exchanged between the two fluids is observed. Therefore, there is an intensification of heat transfer in the presence of low power ultrasound, regardless of the ultrasonic frequency of 45 kHz or 27 kHz. This is confirmed by Tisseau *et al* a systematic increase of the global heat transfer coefficient in the presence of ultrasound which can reach 250% for a tube bundle/calendar type heat exchanger coupled to an ultrasonic field. This improvement does not vary with the power of the ultrasonic field but is very sensitive to the hydrodynamic configuration chosen [30].

This improvement in heat transfer is independent of the thickness of the fouling. At the end of each test, a deposition protocol has been programmed and based on the Ca^{2+} and Mg^{2+} dosage of the washing solution, we can estimate the amount deposited on all the cold compartments of the exchanger. For the transducers, and whatever the power tested, the quantity of deposited limestone does not exceed 1.5 ± 0.2 grams distributed over 10 plates. In order to show the influence of the addition of frequencies on the heat transfer, another series of tests was carried out, but this time in the presence of two transducers programmed on two different frequencies and same ultrasonic power, and which functions at the same time. The applied ultrasonic power is of the order of 15 W. The two transducers were tested at different locations of the exchanger as shown in figure 13.

The variation of the global co-efficient of the exchanger during 72 h operating in multi-frequency and the same power is gathered in figure 14.

To ensure proper operation of the transducers at the same time, the distance between the transducers must be equal to or greater than $\lambda/2$. In our case, for the 27 kHz transducer this ratio is close to 15, and for 45 kHz is about 17. Therefore, the distance between the two transducers is about 17.8 cm. According to the comparison of the obtained results, the best position to expect a better heat transfer is position number 2. This has been confirmed by a study carried out by a study by Nakayama *et al* who indicated that the improvement in heat transfer depended on the positioning of the transducer and also on the flux. According to the authors, the case of low heat flux was better than the case of high heat flux (Nakayama and Kano, n.d.).

On the other hand, this improvement does not exceed the rate of the global exchange coefficient obtained by a single 45 kHz–15 W transducer. This improvement in the transfer is independent of the transfer resistance of

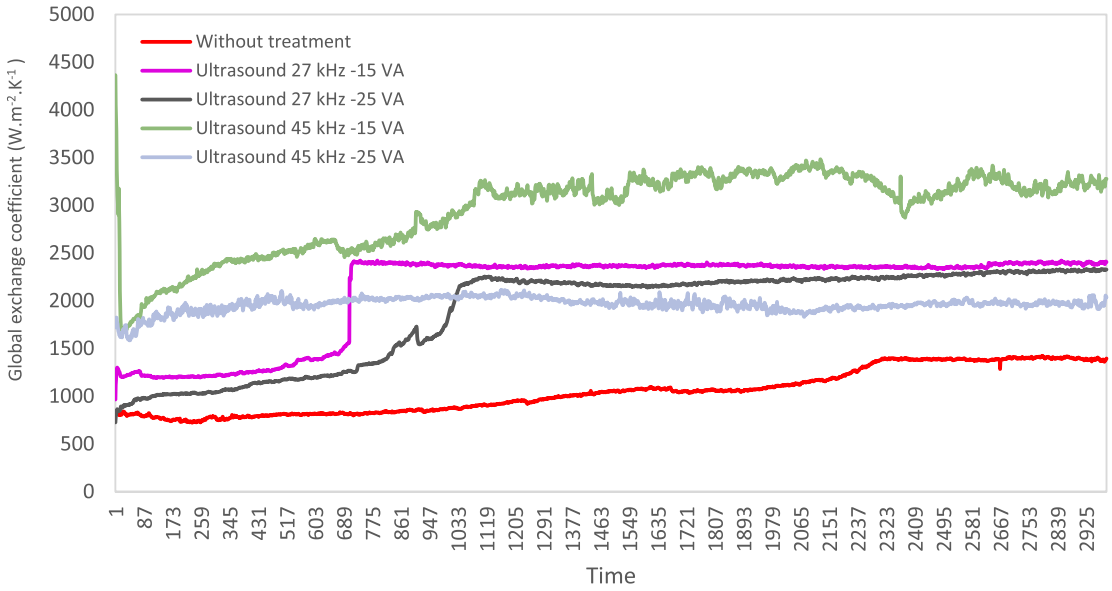

Figure 12. Variation of the global exchange coefficient without and with ultrasound.

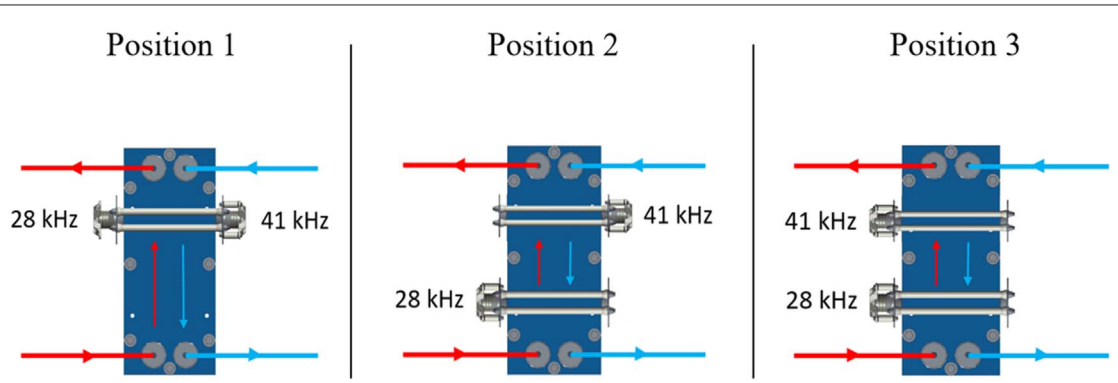

Figure 13. Variation of the positioning of the ultrasonic transducers.

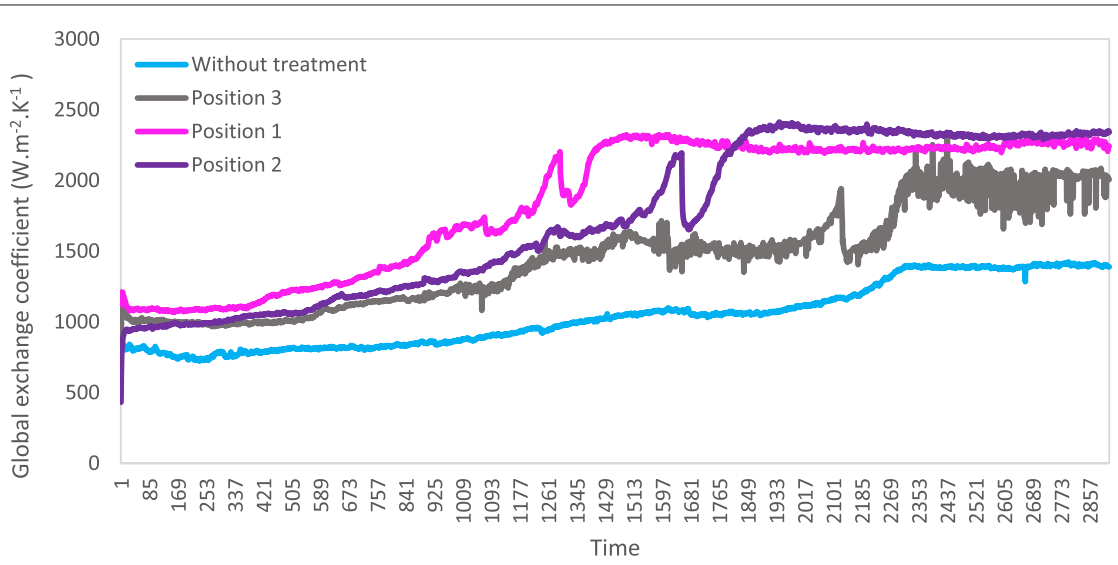

Figure 14. Monitoring the variation of the global exchange coefficient in the presence of multi-frequencies at different locations.

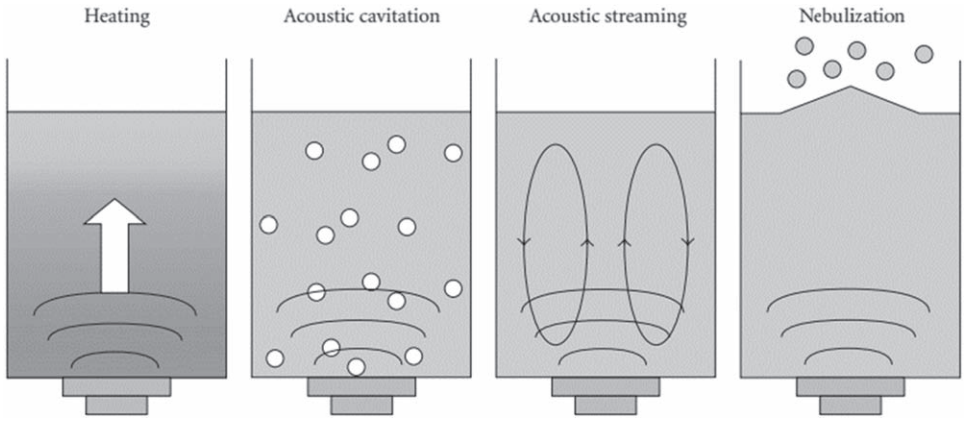

Figure 15. Four effects resulting from ultrasound propagation in a liquid.

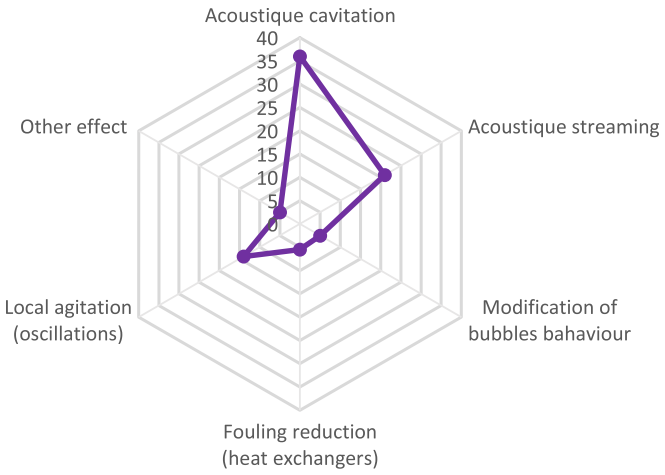

Figure 16. Effects responsible for the improvement of heat transfers [31].

the fouling. The scale deposited on the total exchange surface, which is about 0.38 m^2, does not exceed 0.98 ± 0.05 grams distributed over 10 plates, in all the multi-frequency tests.

The results obtained show that ultrasound can improve heat transfer at different frequencies, at different powers, or in multi-frequency mode. We also found that the overall exchange coefficient is doubled for a frequency of 45 kHz and an ultrasonic power of 15 W. It is well known that the rate of heat transfer from a solid surface to a fluid is increased in an ultrasonic field, but the mechanism of heat transfer enhancement with ultrasound has not been sufficiently elucidated. In order to clarify the mechanism of heat transfer by ultrasonic irradiation.

When emitted ultrasound in liquid several can be induced. First, the liquid can be heated because of the acoustic energy. The dissipation of ultrasound in the liquid can create a momentum gradient, which causes a movement of the fluid, called acoustic current. It can appear micro-bubbles of vapor in the liquid medium, and agitate the liquid at the microscopic level, this phenomenon is called acoustic cavitation. Finally, a fourth phenomenon that can appear, at high frequency only, is the nebulization or the acoustic fountain [19]. Figure 15 shows all these phenomena.

In the presence of ultrasound, the phenomenon of acoustic cavitation is capable of triggering a turbulent transition, which makes ultrasound more apt to intensify heat transfer in the laminar regime [4]. As shown in figure 16.

For the purpose of observing cavitation and thermal bubble behavior using a high-speed video imaging system, Kim *et al* conducted tests that show that the effects of ultrasonic vibrations on flow behavior are very different depending on the heat transfer regime and the amount of dissolved gas. In the natural convection and subcooled boiling regimes, the behavior of cavitation bubbles strongly affects the degree of heat transfer

enhancement. In saturated boiling, no cavitation occurs, so the small size of the thermal bubbles at the start and the acoustic flux are major factors improving the heat transfer rate [32].

Another experimental study was conducted to investigate the effects of acoustic cavitation on natural convection heat transfer from a horizontal circular tube. The experimental results indicate that the rate of heat transfer enhancement increases with the intensity of cavitation [6]. The cavitation enhancement was explained by the turbulence thermal conductivity of the microjets [33].

Cai *et al* numerically studied the heat transfer with and without acoustic cavitation. The simulation results show that the temperature uniformity of the liquid and the heat transfer coefficient of the heating surface are greatly improved using acoustic cavitation [5]. The authors showed in another study that when the heat flow is low, the improvement of heat transfer by acoustic cavitation has a better effect than increasing the cavitation intensity [16].

According to Uhlenwinkel *et al* the phenomenon responsible for the heat transfer enhancement is the acoustic pressure. The authors succeeded in developing an empirical equation to calculate the effective acoustic pressure in the acoustic standing wave field [34].

According to Lee and Loh, the mechanism responsible for the increase in flow velocity is acoustic streaming. The authors were able to visualize by particle imaging velocimetry (PIV) the phenomenon of acoustic streaming induced by longitudinal vibrations at 30 kHz [35]. This is confirmed in an experimental study by Nomura *et al* where they found that the mechanism of heat transfer enhancement by 60.7 kHz and 20 W ultrasonic vibration in tap water is the acoustic current [10].

Conclusion

This work was carried out with the objective of inhibiting the formation of mineral deposits in heat exchangers. The results of the study also show that ultrasound allows an increase in heat transfer. These results are in agreement with the results of the bibliography.

It is thus possible to intensify the heat transfer with low power ultrasonic waves, in order to increase the performance of the exchanger. The objective can be to reduce energy consumption. However, the integration of ultrasonic guided waves in a heat exchanger does not depend only on thermal considerations. Indeed, the sonochemistry of the ultrasonic waves, the hydraulic configuration, the flow regime, the constituent materials, and the mixing properties can also influence the heat exchange quality.

Acknowledgments

The authors would like to thank the Grand-EST region, BPI France and the European Regional Development Fund for their financial support.

Data availability statement

The data that support the findings of this study are available upon reasonable request from the authors.

Author's statements

This study is part of the ExUS project, directed by Dr Hervé MUHR as thesis director. Dr Marie LE PAGE MOSTEFA is co-director of the thesis. Mrs. Nihad KAMAR has carried out the experimental measurements and has written this document. Mr Pierre-Olivier JOST is the project leader.

Financial statement

This work was supported by the [Grand EST region] under Grant [number 19P02300]; [BPI France bank] under Grant [number DOS0097779/00]; and [European Regional Development Fund FEDER] under Grant [number 17SP-2320].

Declaration of competing interests

The authors declare that they have no known competing financial interests or personal relationships that might appear to influence the work reported in this article.

ORCID iDs

Nihad Kamar https://orcid.org/0000-0002-2178-9368

References

[1] Chérif Sadouk H 2010 Modélisation de l'encrassement en régime turbulent dans un échangeur de chaleur à plaques avec un revêtement fibreux sur les parois https://tel.archives-ouvertes.fr/tel-00499251

[2] Andrijić Ž U, Bolf N, Rimac N and Brzović A 2021 Fouling detection in industrial heat exchanger using number of transfer units method, neural network, and nonlinear finite impulse response models *Heat Transf. Eng.* 1–15

[3] Panchal C B and Huangfu E P 2000 Effects of mitigating fouling on the energy efficiency of crude-oil distillation *Heat Transf. Eng.* **21** 3–9

[4] Bulliard-sauret O 2016 'thermiques par les ultrasons en convection forc ´ ee Odin BULLIARD-SAURET Étude expérimentale de l ' intensification des transferts thermiques par les ultrasons en convection forcée,'

[5] Cai J, Huai X, Yan R and Cheng Y 2009 Numerical simulation on enhancement of natural convection heat transfer by acoustic cavitation in a square enclosure *Appl. Therm. Eng.* **29** 1973–82

[6] Nakayama A and Kano M 1990 Enhancement of saturated nucleate pool boiling heat transfer by ultrasonic vibrations *Heat Transf.—Japanese Res. (United States)* **56** 1071–6

[7] Monnot A *et al* 2020 Conception et étude préliminaire d ' un échangeur de chaleur tubes et calandres assisté par Ultrasons 0–6 https://hal.archives-ouvertes.frTo cite this version : HAL Id : hal-00271213

[8] Nomura S, Murakami K, Aoyama Y and Ochi J 1998 Effects of change in frequency of ultrasonic vibrations on heat transfer *Nihon Kikai Gakkai Ronbunshu, B Hen/Transactions Japan Soc. Mech. Eng. Part B* **4** 1832–8

[9] Nomura S, Nakagawa M, Mukasa S, Toyota H, Murakami K and Kobayashi R 2005 Ultrasonic heat transfer enhancement with obstacle in front of heating surface *Jpn. J. Appl. Phys.* **44** 4674–7

[10] Nomura S, Yamamoto A and Murakami K 2002 Ultrasonic heat transfer enhancement using a horn-type transducer *Jpn. J. Appl. Phys.* **41** 3217–22

[11] Bartoli C and Baffigi F 2009 Heat transfer enhancement from a circular cylinder to distilled water by ultrasonic waves in subcooled boiling conditions *Proc. ITP2009 Interdiscip. Transp. Phenom. VI Fluid, Therm. Biol. Mater. Sp. Sci.*

[12] Monnot A, Boldo P, Gondrexon N and Bontemps A 2007 Enhancement of cooling rate by means of high frequency ultrasound *Heat Transf. Eng.* **28** 3–8

[13] Gondrexon N, Rousselet Y, Legay M, Boldo P, Le Person S and Bontemps A 2010 Intensification of heat transfer process: improvement of shell-and-tube heat exchanger performances by means of ultrasound *Chem. Eng. Process. Process Intensif.* **49** 936–42

[14] Hoshino T and Yukawa H 1979 Physical mechanism of heat transfer from heated and cooled cylinder to water in ultrasonic standing wave field *J. Chem. Eng. Japan* **12** 347–52

[15] Komarov S and Hirasawa M 2003 Enhancement of gas phase heat transfer by acoustic field application *Ultrasonics* **41** 289–93

[16] Cai J, Huai X, Liang S and Li X 2010 Augmentation of natural convective heat transfer by acoustic cavitation *Front. Energy Power Eng. China* **4** 313–8

[17] Bonekamp S and Bier K 1997 Influence of ultrasound on pool boiling heat transfer to mixtures of the refrigerants R23 and R134A *Int. J. Refrig* **20** 606–15

[18] Legay M, Simony B, Boldo P, Gondrexon N, Le Person S and Bontemps A 2012 Improvement of heat transfer by means of ultrasound: application to a double-tube heat exchanger *Ultrason. Sonochem.* **19** 1194–200

[19] Mathieu L 2012 'Intensification des processus de transfert de chaleur par ultrasons , vers un nouveau type d ' échangeur de chaleur : l ' échangeur vibrant,', doi: https://tel.archives-ouvertes.fr/tel-00848254 Unpublished on 25 Jul 2013 HAL

[20] Markov A V, Astashkin Y S and Sulimtsev I I 1985 Influence of ultrasound on heat transfer under the conditions of forced flow of a high-temperature melt *J. Eng. Phys.* **48** 242–4

[21] KAMAR N, Mostefa M L P, Muhr M H and Jost P O 2022 Scaling control by using ultrasonic guided waves *Chem. Eng. Process. - Process Intensif.* **176** 108969

[22] Kamar N, Le page Mostefa M, Muhr H and Jost P 2022 Identification of areas susceptible to calcium carbonate formation on a surface of a plate and gasket heat exchanger *Chem. Eng. Commun.* **0** 1–12

[23] Pétrier C, Gondrexon N and Boldo P 2008 Ultrasons et sonochimie *Tech. L'Ingénieur* **AF6310** 14

[24] Corrieu G, Lalande M and Ferret R 1986 Mesure en ligne de l'encrassement et du nettoyage d'un sterilisateur UHT industriel *J. Food Eng.* **5** 231–48

[25] Jradi R, Fguiri A, Marvillet C and Jeday M R 2019 Experimental analysis of heat transfer coefficients in phosphoric acid concentration process *J. Stat. Mech: Theory Exp.* **2019** 84002

[26] Fguiri A, Marvillet C and Jeday M R 2021 Estimation of fouling resistance in a phosphoric acid/steam heat exchanger using inverse method *Appl. Therm. Eng.* **192** 116935

[27] Heat exchangers, France Che. ENSIC-Nancy 2002

[28] Pátek J, Hrub J, Klomfar J, Součková M and Harvey A H 2009 Reference correlations for thermophysical properties of liquid water at 0.1 MPa *J. Phys. Chem. Ref. Data* **38** 21–9

[29] Sabine R 2019 *Multiphase Operations in Process Engineering: Hydrodynamics, Transfers, Reactions, Mechanical Separations* (Paris: Ellipses)

[30] Tisseau Y, Boldo P, Gondrexon N and Bontemps A 2007 Conception et étude préliminaire d'un échangeur de chaleur tubes et calandre assisté par ultrasons *Proc. 18ème Congrès Fr. Mécanique* pp 27–31

[31] Legay M, Gondrexon N, Le Person S, Boldo P and Bontemps A 2011 Enhancement of heat transfer by ultrasound: review and recent advances *Int. J. Chem. Eng.* **2011** 670108

[32] Kim H-Y, Kim Y G and Kang B H 2003 Enhancement of natural convection and pool boiling heat transfer via ultrasonic vibration *Heat Transfer Summer Conf. (ASME 2003) (Las Vegas, Nevada, USA, July 21–23, 2003)* (Digital Collection: ASME) pp 295–302

[33] Nomura S and Nakagawa M 1993 Ultrasonic enhancement of heat transfer on narrow surface *Heat Transf.* **22** 546–58

[34] Uhlenwinkel V, Meng R and Bauckhage K 2000 Investigation of heat transfer from circular cylinders in high power 10 kHz and 20 kHz acoustic resonant fields *Int. J. Therm. Sci.* **39** 771–9

[35] Lee D-R and Loh B-G 2007 Smart cooling technology utilizing acoustic streaming *IEEE Trans. Components Packag. Technol.* **30** 691–9